Two oxo complexes with tetra-nuclear [Fe$_4$(μ_3-O)$_2$]$^{8+}$ and trinuclear [Fe$_3$(μ_3-O)]$^{7+}$ units

Piedad Cortés,[a]* Ana María Atria,[a,b] María Teresa Garland[b,c] and Ricardo Baggio[d]

[a]Facultad de Ciencias Químicas y Farmacéuticas, Universidad de Chile, Santiago, Chile, [b]CIMAT, Universidad de Chile, Santiago, Chile, [c]Departamento de Física, Facultad de Ciencias Físicas y Matemáticas, Universidad de Chile, Santiago, Chile, and [d]Departamento de Física, Comisión Nacional de Energía Atómica, Buenos Aires, Argentina
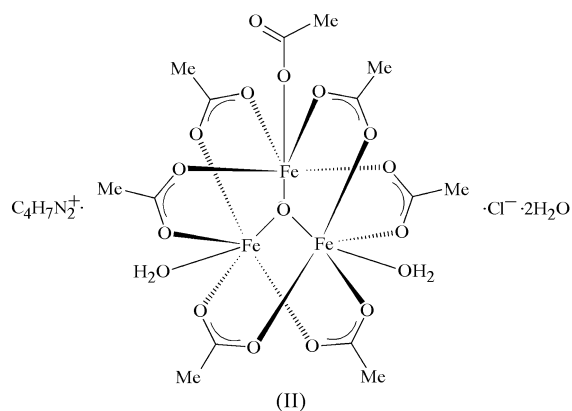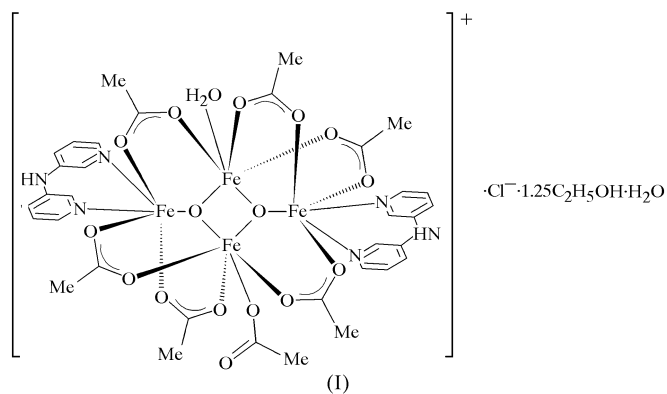
Correspondence e-mail: pcortes@ciq.uchile.cl

As a contribution to the general understanding of oxo-bridged polynuclear iron complexes, we present here the crystal structures of two oxo-bridged Fe^{III} ionic complexes, viz. [Fe$_4$(CH$_3$COO)$_7$O$_2$(BPA)$_2$(H$_2$O)]$^+$·Cl$^-$·1.25CH$_3$CH$_2$OH·-H$_2$O (BPA is di-3-pyridylamine), (I), and MeImid$^+$·[Fe$_3$-(CH$_3$COO)$_7$O(H$_2$O)$_2$]·Cl$^-$·2H$_2$O, (II) (MeImid$^+$ is 2-methyl-imidazolium).

(I)

(II)

Two new oxo complexes, namely hexa-μ_2-acetato-acetato-aquabis(di-3-pyridylamine)di-μ_3-oxo-tetrairon(III) chloride monohydrate ethanol 1.25-solvate, [Fe$_4$(C$_2$H$_3$O$_2$)$_7$O$_2$(C$_{10}$H$_9$-N$_3$)$_2$(H$_2$O)]Cl·1.25C$_2$H$_6$O·H$_2$O, (I), containing a tetranuclear [Fe$_4$(μ_3-O)$_2$]$^{8+}$ unit, and 2-methylimidazolium hexa-μ_2-acetato-acetatodiaqua-μ_3-oxo-triiron(III) chloride dihydrate, (C$_4$H$_7$N$_2$)[Fe$_3$(C$_2$H$_3$O$_2$)$_7$O(H$_2$O)$_2$]Cl·2H$_2$O, (II), with a trinuclear [Fe$_3$(μ_3-O)]$^{7+}$ unit, are presented. Both structures are formed by two well differentiated entities, viz. a compact isolated cluster composed of Fe^{III} ions coordinated to O^{2-} and CH$_3$CO$_2^-$ anions, and an external group formed by a central Cl$^-$ ion surrounded by different solvent groups to which the anion is bound through hydrogen bonding. In the case of (I), charge balance cannot be achieved within the groups, so the structure is macroscopically ionic; in the case of (II), in contrast, each group is locally neutral owing to the internal compensation of charges. The trinuclear complex crystallizes with the metal cluster, chloride anion and 2-methyl-imidazolium cation bisected by a crystallographic mirror plane.

Comment

Molecules containing one or more oxo-bridged Fe atoms have been the subject of extensive investigation in a variety of contexts, viz. biological [owing to the fact that polynuclear oxo-bridged Fe^{III} units are frequently found in the active sites of different proteins (Gilles et al., 2002)], technological [as in the design of new molecule-based magnets (Podgajny et al., 2002; Marchivie et al., 2002; Sokol et al., 2002; Larrionava et al., 2000)], physico-chemical {valence trapping problems in mixed valence [Fe^{II}Fe$_2^{III}$O]$^{6+}$ trinuclear carboxylate complexes (Oh et al., 1984; Woehler et al., 1987)], etc.

In a general overview, the two structures can be defined as similar in their gross features, being formed by isolated clusters composed of Fe^{III} ions coordinated to O^{2-} and acetate anions, stabilized by an external group of different solvent species having a central Cl$^-$ ion to which they attach through a variety of hydrogen-bonding interactions (see below).

A charge-balance analysis, however, shows the structures to be rather different in that the metal cluster in (I) does not balance the 12 positive charges furnished by the metal ions with the 11 negative charges provided by the anions (two oxo and seven acetate units). The result is a singly charged cationic cluster externally balanced by a Cl$^-$ anion. The cluster in (II), however, is neutral owing to the presence of three Fe^{3+} ions on one hand, and one O^{2-} and seven acetate ions on the other; the external part, in turn, also presents electrostatic balance with the Cl$^-$ ion hydrogen bonded to an MeImid$^+$ group.

In addition to the Coulomb forces present, both group types interact with each other via hydrogen bonding through a definite number of hydrogen bonding 'active sites'. Figs. 1 and 2 show complete views of both structures in terms of this latter description, while Figs. 3 and 4 show schematic sketches of the corresponding metal clusters. It can be readily seen that each
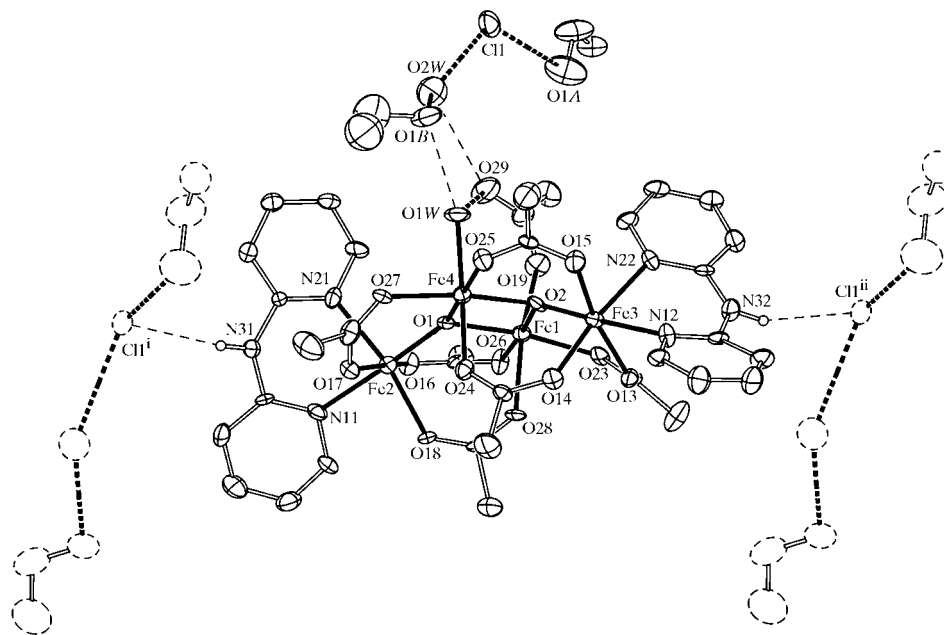
Figure 1
A molecular ellipsoid plot of (I) (30% probability level), showing the complete tetrameric cation and the three symmetry-related 'anionic groups' hydrogen bonded to it. Independent atoms are drawn with principal axis displacement ellipsoids, while their symmetry-related counterparts are shown as open ellipsoids. Heavy broken lines denote interactions internal to the 'anionic groups' and light broken lines denote those involving the cation. C atoms are not labelled for clarity. The symmetry codes are as in Table 2.
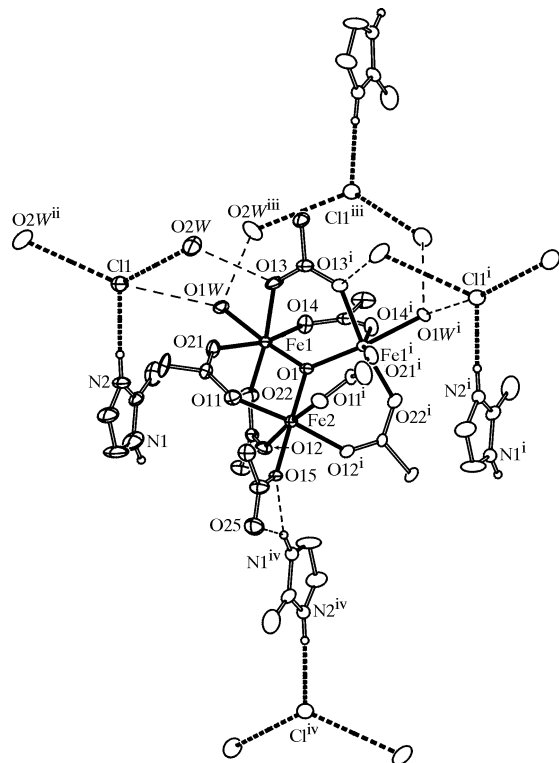

Figure 2
A molecular ellipsoid plot of (II) (30% probability level), showing the complete trimeric cation and the four symmetry-related 'anionic groups' hydrogen bonded to it. Independent atoms are drawn with principal axis displacement ellipsoids, while their symmetry-related counterparts are shown as open ellipsoids. Heavy broken lines denote interactions internal to the 'anionic groups' and light broken lines denote those involving the cation. C atoms are not labelled for clarity. [Symmetry codes: (i) $x, -y + \frac{3}{2}, z$; (ii) $x, -y + \frac{1}{2}, z$; (iii) $-x + \frac{1}{2}, -y + 1, z + \frac{1}{2}$; (iv) $-x, -y + 1, -z + 2$.]

of the general organizational features mentioned so far is achieved in each structure in a different way, according to the number and nature of their ligands/solvent species. We shall now describe this in detail.

In compound (I), the isolated cationic clusters are composed of four Fe^{III} cations, coordinated to two O^{2-} groups, seven acetate anions, two BPA bases and one water molecule. The internal charge balance gives a net cationic charge of +1.

The cation comprises an innermost core of two Fe atoms (Fe1 and Fe4) doubly bridged by atoms O1 and O2, the oxo units, which in turn connect outwards to the remaining Fe atoms (one each), Fe2 and Fe3, to fulfill their μ_3-coordination. To these outermost Fe atoms, the trinitrogenated BPA bases chelate *via* pyridyl atoms N11 and N12, and N21 and N22, respectively. Adjacent Fe atoms are in turn connected by a different number of acetate bridges. The pairs Fe1/Fe2 and Fe3/Fe4 are doubly bridged by acetate ions Ac6/Ac8 and Ac4/Ac5, respectively (where Acx denotes the acetate ion containing atoms O1x and O2x), while the pairs Fe1/Fe3 and Fe4/Fe2 are singly bridged by ions Ac3 and Ac7, respectively. The central pair, Fe1/Fe4, is the only exception to this rather symmetric coordination, their bridging being achieved through a larger hydrogen-bonded loop involving Ac9 (singly bound to Fe1) and aqua atom O1W, bound to atom Fe4. As a consequence of the tight binding resulting from this latter bridge and the double oxo bridges, there is a rather short Fe1···Fe4 distance in the innermost Fe_2O_2 loop [2.924 (1) Å], a value in the lower seventh percentile of homologous distances reported for similar loops in the November 2005 version of the Cambridge Structural Database (CSD; Allen, 2002).

All four iron environments are slightly distorted octahedral; as a measure of this distortion, the maximum deviations from the ideal 180° angles are 14.7 (2), 12.95 (19), 12.65 (19) and 9.5 (2)°, respectively, for the sequence Fe1–Fe4.

The Fe—O bond distances also exhibit differences, but with similarly coordinated cations showing analogous trends; thus, the environments for the Fe1/Fe4 pair are alike, as are those for Fe2/Fe3.

The first group (Fe1/Fe4) is characterized by three sets of rather similar bond lengths [short, medium and long, with mean values of 1.95 (3), 1.99 (2) and 2.06 (2) Å, respectively; Table 1], the first corresponding to the oxo bonds and the other two showing no obvious characteristic telling them apart. The second group also has three sets of distances, the oxo distances being by far the shortest [mean = 1.825 (5) Å], the remaining acetate O atoms forming the second [mean = 2.027 (9) Å] and finally the BPA N atoms the third [mean = 2.17 (2) Å].

The six chelating acetate groups exhibit rather erratic behaviour regarding delocalization of the double bond, as inferred from the differences in their C—O distances, which range from some 0.3% of their mean value (almost complete delocalization) climbing to 9.5% (almost a pure single/double bond situation). Even though this is a rather extreme case for a chelating acetate ligand, it is by no means unique; we could trace in the CSD chelating acetate ligands with asymmetries as large as 10.2% (CSD code ACENOL). The singly coordinated
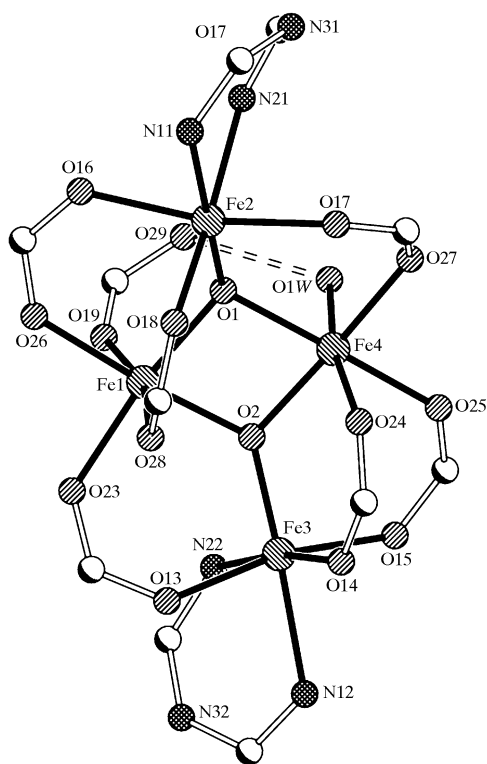
Ac9 ion seems to lie somewhere in between the two extreme cases, with a 3.7% difference.

The stabilizing 'anionic group' in (I) consists of a chloride anion and three solvent molecules [one water and two depleted ethanol sites, with site-occupation factors of 0.52 (2) and 0.73 (2), these latter four molecules strongly linked to each other through hydrogen bonding into a unique rather 'linear' entity, as shown in Fig. 1].
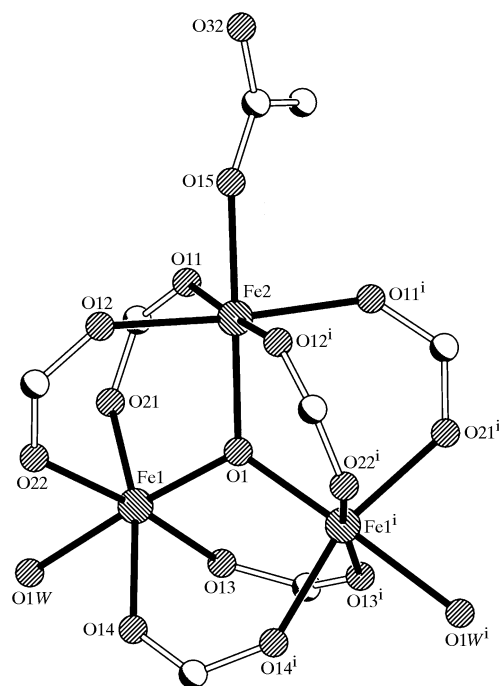
Figure 4
A schematic view of the trimeric core in (II), with H and some C atoms omitted for clarity.
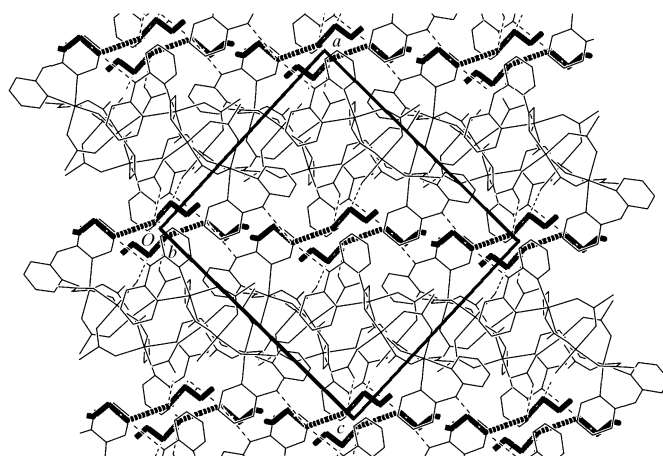
Figure 5
A packing plot of (I), viewed along b, showing the way in which both cationic and anionic groups form sheets parallel to (10$\bar{1}$), the anions (in bold lines) passing through the cell centre and the cations (in light lines) lying immediately above/below the cell centre.

Figure 3
A schematic view of the tetrameric core in (I), with H and some C atoms omitted for clarity. Double dashed lines denote the intramolecular hydrogen bond connecting atom O1W and Ac9.

In spite of the fact that H atoms attached to O atoms could not be found confidently in the difference Fourier map, a plausible interaction scheme can be envisaged from the short $D\cdots A$ distances between the two clusters.

The cationic group has three different active sites (Fig. 1), represented by amine atoms N31 and N32 (acting as donors), the set composed of aqua ligand O1W (acting as a donor), and the uncoordinated carboxylate atom O29, a double acceptor of both an intermolecular hydrogen bond from O2W in the anionic group and the only intramolecular hydrogen bond in the cation, from O1W (entries 1–5 in Table 2).

The anionic group, in turn, has three weak internal interactions attributable to hydrogen bonding and contributing to its internal coherence (entries 6–8 in Table 2).

The final result is a packing structure composed of cationic and anionic sheets parallel to $(10\bar{1})$, as shown in Fig. 5.

In the case of (II), the isolated metal clusters are composed of three Fe^{III} cations, centrally coordinated by a single O^{2-} group, seven acetate anions and two water molecules, producing a neutral environment around the metal atom.

The group is, however, much more symmetric than its counterpart in (I), being bisected by a mirror plane that passes though one of the Fe atoms (Fe2) and the central oxo O1 atom, and which bisects ions Ac3, Ac4 and Ac5.

The innermost core consists of the Fe_3O group. In addition to this oxo bridging, all pairs of Fe atoms are doubly bridged by acetate anions, as follows: atoms Fe1 and Fe2 by ions Ac1 and Ac2, and atoms Fe1 and Fe1^{i} by ions Ac3 and Ac4 [symmetry code: (i) $x, \frac{3}{2} - y, z$]. Finally, atom Fe1 (Fe1^{i}) coordinates to aqua ligand O1W (O1W^{i}), while atom Fe2 binds to the monocoordinated ion Ac5. This completes the distorted octahedral environment for each Fe atom (Table 3, and Figs. 2 and 4).

Though to a lesser degree than in (I), the six chelating acetate groups also display a variety of double-bond behaviours, from perfect 100% delocalization in the symmetric Ac3 and Ac4 ions, up to larger differences, as in Ac2 (4.2%). The singly coordinated Ac5 ion has an asymmetry of 3.4%.
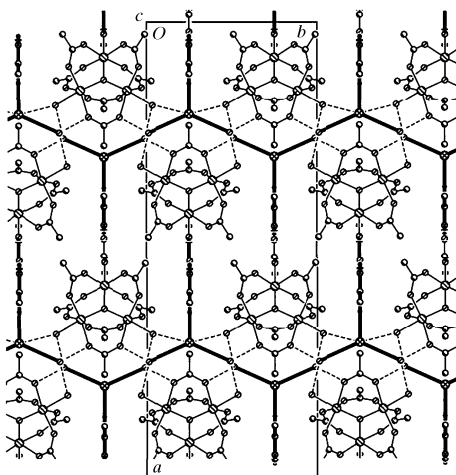

Figure 6
A packing plot of (II), viewed along c, showing the anionic cages (bolder lines) in which the cationic groups (lighter lines) lodge.

The 'solvate part' in (II) lies, as the iron cluster does, on a symmetry plane passing through Cl1^{-} and the MeImid^{+} cation. The ensemble is completed by two hydration water molecules (atoms O2W and O2W^{ii} in Fig. 2), one on each side of the plane.

As with (I), we were unable to find the H atoms involved in hydrogen-bonding interactions in (II), but here again the interaction scheme could be ascertained from the short $D\cdots A$ distances between the clusters. In this case, the cationic group has five active sites (see Fig. 2), represented by atom O1W as a double donor, atom O13 as an acceptor, and lastly atoms O15 and O25 as joint acceptors of a single bifurcated interaction with the N1—H1 group (entries 3–7 in Table 4). The anionic group, in turn, is stabilized by two internal hydrogen bonds to Cl1 (entries 1 and 2 in Table 4).

The resulting packing scheme is a three-dimensional structure composed of anionic cages in which the cations lodge (Fig. 6).

Experimental

The syntheses were performed according to the procedure reported by McCuster *et al.* (1991). However, only in the case of (I) did the corresponding amine (BPA) appear, as expected, in a coordinated mode. In the case of (II), the MeImid^{+} group did not bind to the cation. For the preparation of (I) and (II) sodium acetate (6.63 mmol) and 1.43 mmol of the respective amine, *viz.* BPA in the case of (I) and MeHImid in that of (II), were added to an orange solution of $FeCl_3\cdot 6H_2O$ (2.67 mmol) in ethanol (50 ml). The resulting solutions were stirred at room temperature for 10 min. Following the literature method, an excess of $KClO_4$ was added to the reaction mixtures, and the resulting solutions were stirred overnight at room temperature. In both cases, a fine red–brown solid was collected by filtration. Recrystallization from an EtOH/Et$_2$O mixture provided the poorly diffracting crystals used for data collection.

Compound (I)

Crystal data

$[Fe_4(C_2H_3O_2)_7O_2(C_{10}H_9N_3)_2(H_2O)]Cl\cdot 1.25C_2H_6O\cdot H_2O$	$V = 5070\ (2)$ Å^3
$M_r = 1140.18$	$Z = 4$
Monoclinic, $P2_1/n$	$D_x = 1.494$ Mg m^{-3}
$a = 16.044\ (4)$ Å	Mo $K\alpha$ radiation
$b = 17.619\ (4)$ Å	$\mu = 1.25$ mm^{-1}
$c = 17.942\ (5)$ Å	$T = 295\ (2)$ K
$\beta = 91.571\ (5)°$	Plate, red
	$0.23 \times 0.15 \times 0.08$ mm

Data collection

Bruker SMART CCD area-detector diffractometer	20171 measured reflections
φ and ω scans	8964 independent reflections
Absorption correction: multi-scan (*SADABS*; Sheldrick, 2001)	4931 reflections with $I > 2\sigma(I)$
$T_{min} = 0.79$, $T_{max} = 0.90$	$R_{int} = 0.072$
	$\theta_{max} = 25.2°$

Refinement

Refinement on F^2	H-atom parameters constrained
$R[F^2 > 2\sigma(F^2)] = 0.068$	$w = 1/[\sigma^2(F_o^2) + (0.0623P)^2]$
$wR(F^2) = 0.160$	where $P = (F_o^2 + 2F_c^2)/3$
$S = 1.01$	$(\Delta/\sigma)_{max} = 0.007$
8964 reflections	$\Delta\rho_{max} = 0.48$ e Å^{-3}
635 parameters	$\Delta\rho_{min} = -0.50$ e Å^{-3}

Table 1
Selected bond lengths (Å) for (I).

Fe1—O1	1.933 (4)	Fe3—O14	2.041 (5)
Fe1—O2	1.956 (5)	Fe3—N12	2.176 (6)
Fe1—O19	1.971 (5)	Fe3—N22	2.198 (5)
Fe1—O23	1.996 (5)	Fe4—O2	1.915 (4)
Fe1—O26	2.044 (5)	Fe4—O1	1.986 (5)
Fe1—O28	2.082 (4)	Fe4—O27	2.000 (5)
Fe2—O1	1.820 (4)	Fe4—O25	2.006 (5)
Fe2—O16	2.024 (5)	Fe4—O1W	2.054 (5)
Fe2—O17	2.028 (5)	Fe4—O24	2.055 (5)
Fe2—O18	2.035 (4)	Fe1—Fe2	3.3335 (16)
Fe2—N21	2.145 (5)	Fe1—Fe3	3.4134 (16)
Fe2—N11	2.175 (5)	Fe1—Fe4	2.9243 (16)
Fe3—O2	1.828 (4)	Fe2—Fe4	3.4199 (17)
Fe3—O13	2.016 (5)	Fe3—Fe4	3.2990 (16)
Fe3—O15	2.021 (5)		

Table 2
Hydrogen-bond geometry (Å, °) for (I).

$D—H\cdots A$	$D—H$	$H\cdots A$	$D\cdots A$	$D—H\cdots A$
N31—H31N$\cdots$Cl1^i	0.86	2.48	3.221 (6)	145
N32—H32N$\cdots$Cl1^{ii}	0.86	2.45	3.246 (6)	154
O1W$\cdots$O29	–	–	2.534 (9)	–
O1W$\cdots$O1B	–	–	2.618 (10)	–
O2W$\cdots$O29	–	–	2.765 (14)	–
O2W$\cdots$Cl1	–	–	3.196 (8)	–
O1A$\cdots$Cl1	–	–	3.313 (15)	–
O1B$\cdots$O2W	–	–	2.774 (11)	–

Symmetry codes: (i) $x + \frac{1}{2}, -y + \frac{3}{2}, z - \frac{1}{2}$; (ii) $x + \frac{1}{2}, -y + \frac{3}{2}, z + \frac{1}{2}$.

Compound (II)

Crystal data

$(C_4H_7N_2)[Fe_3(C_2H_3O_2)_7O-(H_2O)_2]Cl\cdot 2H2O$	$Z = 4$
$M_r = 787.49$	$D_x = 1.675$ Mg m^{-3}
Orthorhombic, $Pnma$	Mo $K\alpha$ radiation
$a = 32.147$ (6) Å	$\mu = 1.54$ mm^{-1}
$b = 12.048$ (2) Å	$T = 295$ (2) K
$c = 8.0652$ (16) Å	Block, red
$V = 3123.6$ (11) Å^3	$0.26 \times 0.25 \times 0.20$ mm

Data collection

Bruker SMART CCD area-detector diffractometer	5673 measured reflections
	2877 independent reflections
φ and ω scans	1584 reflections with $I > 2\sigma(I)$
Absorption correction: multi-scan ($SADABS$; Sheldrick, 2001)	$R_{int} = 0.079$
	$\theta_{max} = 25.0°$
$T_{min} = 0.68, T_{max} = 0.73$	

Refinement

Refinement on F^2	$w = 1/[\sigma^2(F_o^2) + (0.0993P)^2$
$R[F^2 > 2\sigma(F^2)] = 0.069$	$+ 17.3868P]$
$wR(F^2) = 0.223$	where $P = (F_o^2 + 2F_c^2)/3$
$S = 1.01$	$(\Delta/\sigma)_{max} = 0.013$
2877 reflections	$\Delta\rho_{max} = 0.89$ e Å^{-3}
225 parameters	$\Delta\rho_{min} = -0.79$ e Å^{-3}
H-atom parameters constrained	

H atoms attached to C and N atoms were placed at calculated positions (N—H = 0.86 Å, aromatic C—H = 0.93 Å and methyl C—H = 0.96 Å) and allowed to ride. Even though located in a poorly defined, rather shallow, electron-density plateau, H atoms from the methyl groups were also included [AFIX 137 in *SHELXL97* (Sheldrick, 1997)] because of their incidence in the refinement. H atoms attached to O atoms, however, were excluded, because they could not

Table 3
Selected bond lengths (Å) for (II).

Fe1—O1	1.894 (3)	Fe2—O1	1.950 (6)
Fe1—O14	1.996 (5)	Fe2—O15	1.988 (6)
Fe1—O21	2.009 (5)	Fe2—O11	2.029 (5)
Fe1—O22	2.009 (5)	Fe2—O12	2.042 (5)
Fe1—O13	2.062 (5)	Fe1—Fe1^i	3.298 (2)
Fe1—O1W	2.118 (5)	Fe1—Fe2	3.321 (2)

Symmetry code: (i) $x, -y + \frac{3}{2}, z$.

Table 4
Hydrogen-bond geometry (Å, °) for (II).

$D—H\cdots A$	$D—H$	$H\cdots A$	$D\cdots A$	$D—H\cdots A$
N2—H2N$\cdots$Cl1	0.86	2.24	3.094 (13)	174
O2W$\cdots$Cl1	–	–	3.315 (9)	–
O1W$\cdots$Cl1	–	–	3.323 (8)	–
O1W$\cdots$O2W^{iii}	–	–	2.651 (11)	–
O2W$\cdots$O13	–	–	2.910 (13)	–
N1—H1N$\cdots$O15^{iv}	0.86	2.03	2.826 (12)	154
N1—H1N$\cdots$O25^{iv}	0.86	2.38	3.132 (12)	146

Symmetry codes: (iii) $-x + \frac{1}{2}, -y + 1, z + \frac{1}{2}$; (iv) $-x, -y + 1, -z + 2$.

be located confidently from the difference Fourier syntheses. It was therefore preferred to derive a hydrogen-bonding description mainly in terms of short O$\cdots$O/O$\cdots$N contacts. All H atoms included were assigned a U_{iso}(H) value of xU_{eq}(carrier), with $x = 1.2$ for aromatic H atoms and $x = 1.5$ for methyl H atoms. The quality of the crystals obtained was extremely poor and only with rather long measurement times (20 and 25 s per frame, respectively) was it possible to account for an observed/unique ratio larger than 0.5 (about 0.55 in both cases).

For both compounds, data collection: *SMART-NT* (Bruker, 2001); cell refinement: *SAINT-NT* (Bruker, 2000); data reduction: *SAINT-NT*; program(s) used to solve structure: *SHELXS97* (Sheldrick, 1997); program(s) used to refine structure: *SHELXL97* (Sheldrick, 1997); molecular graphics: *XP* in *SHELXTL-NT* (Bruker, 2000); software used to prepare material for publication: *SHELXL97*.

Supplementary data for this paper are available from the IUCr electronic archives (Reference: FA3019). Services for accessing these data are described at the back of the journal.

References

Allen, F. H. (2002). *Acta Cryst.* B**58**, 380–388.
Bruker (2000). *SAINT-NT* (Version 6.02a) and *SHELXTL-NT* (Version 6.10). Bruker AXS Inc., Madison, Wisconsin, USA.
Bruker (2001). *SMART-NT*. Version 5.624. Bruker AXS Inc., Madison, Wisconsin, USA.
Gilles, C., Bonville, P., Rakoto, H., Broto, J. M., Wong, K. K. W. & Mann, S. (2002). *J. Magn. Magn. Mater.* **241**, 430–440.

Larrionava, J., Gross, M., Pilkington, M., Andres, H., Stoecki-Evans, H., Güdel, H. V. & Decurtins, S. (2000). *Angew. Chem. Int. Ed.* **39**, 1605–1609.

McCuster, J., Vincent, J. B., Schmitt, E. A., Mino, M. L., Shin, K., Coggin, D. K., Hagen, P. M., Huffman, J. C., Christou, G. & Hendrickson, D. N. (1991). *J. Am. Chem. Soc.* **113**, 3012–3021.

Marchivie, M., Guionneau, P., Howard, J. A. K., Chastanet, G., Letard, J.-F., Goeta, A. E. & Chasseau, D. (2002). *J. Am. Chem. Soc.* **124**, 194–195.

Oh, S. M., Hendrickson, D. N., Hasset, K. L. & Davis, R. E. (1984). *J. Am. Chem. Soc.* **106**, 7984–7985.

Podgajny, R., Desplanches, C., Sieklucka, B., Sessoli, R., Villar, V., Paulsen, C., Wernsdorfer, W., Dromzee, Y. & Verdaguer, M. (2002). *Inorg. Chem.* **41**, 1323–1327.

Sheldrick, G. (1997). *SHELXL97* and *SHELXS97*. University of Göttingen, Germany.

Sheldrick, G. M. (2001). *SADABS*. University of Göttingen, Germany.

Sokol, J. J., Hee, A. G. & Long, J. R. (2002). *J. Am. Chem. Soc.* **124**, 7656–7657.

Woehler, S. E., Wittebort, R. J., Oh, S. M., Kambara, T., Hendrickson, D. N., Inniss, D. & Strouse, C. E. (1987). *J. Am. Chem. Soc.* **109**, 1063–1072.